Homotopy Continuation for Spatial Interference Alignment in Arbitrary MIMO X Networks

Jacobo Fanjul, *Student Member, IEEE,* Óscar González, Ignacio Santamaria, *Senior Member, IEEE,* and Carlos Beltrán

***Abstract*—In this paper we propose an algorithm to design interference alignment (IA) precoding and decoding matrices for arbitrary MIMO X networks. The proposed algorithm is rooted in the homotopy continuation techniques commonly used to solve systems of nonlinear equations. Homotopy methods find the solution of a target system by smoothly deforming the solution of a start system which can be trivially solved. Unlike previously proposed IA algorithms, the homotopy continuation technique allows us to solve the IA problem for both unstructured (i.e., generic) and structured channels such as those that arise when time or frequency symbol extensions are jointly employed with the spatial dimension. To this end, we consider an extended system of bilinear equations that include the standard alignment equations to cancel the interference, and a new set of bilinear equations that preserve the desired dimensionality of the signal spaces at the intended receivers. We propose a simple method to obtain the start system by randomly choosing a set of precoders and decoders, and then finding a set of channels satisfying the system equations, which is a linear problem. Once the start system is available, standard prediction and correction techniques are applied to track the solution all the way to the target system. We analyze the convergence of the proposed algorithm and prove that, for many feasible systems and a sufficiently small continuation parameter, the algorithm converges with probability one to a perfect IA solution. The simulation results show that the proposed algorithm is able to consistently find solutions achieving the maximum number of degrees of freedom (DoF) in a variety of MIMO X networks with or without symbol extensions. Further, the algorithm provides insights into the feasibility of IA in MIMO X networks for which theoretical results are scarce.**

***Index Terms*—Degrees of freedom, homotopy continuation, interference alignment, MIMO X networks, feasibility.**

I. Introduction

THE key idea of interference alignment (IA) consists of designing precoding matrices that reduce the dimension of the interference subspace, in such a way that it can be zero-forced by applying the decoding matrices at the receivers. The concept originated from the study of the degrees of freedom (DoF) for the 2-user X channel [2], [3] and the K-user interference channel (IC) [4]. More generally, an $M \times N$ multiple-input multiple-output (MIMO) X network (XN) represents the most general single-hop network model with M transmitters and N receivers, each of them equipped with multiple antennas. Many other well-known network topologies such as the interference channel (IC), the interference multiple-access channel (IMAC), the interference broadcast channel (IBC) and the X channel, can be viewed as particular cases of X networks.

A large number of IA algorithms have been proposed for the IC when the channels are generic, which happens for instance when the channel coefficients are drawn from a continuous distribution and hence the MIMO channel matrices have no particular structure. Widely known examples are the alternating minimization algorithm in [5], [6], as well as the rank minimization method in [7]. Many other algorithms using different cost functions (mean-squared error, average sum-rate) [8], [9], or applying different optimization criteria have been proposed for this particular network topology [10]–[13]. More recently, a Gauss-Newton IA method was proposed in [14] to improve the convergence speed of previous approaches.

On the other hand, when time or frequency symbol extensions are used together with the spatial dimension, the resulting MIMO channels are not generic anymore and therefore specific IA algorithms that preserve the rank of the desired signal subspaces are needed. A couple of examples are the methods in [15], [16], which are applicable only to the IC.

Regarding the application of IA schemes to cellular networks, outer bounds for the DoF of IMAC and IBC networks have been derived in [17]. IA algorithms for cellular networks have been proposed in [18], [19]. Also, the sum-rate performance of IA under imperfect channel state information (CSI) for the IBC is studied in [20]. More recently, the focus has been shifted to the study of the so-called heterogeneous networks (HetNets) [21]. Although work in this area is still scarce, some techniques to obtain IA solutions in HetNets have already been developed. For instance, [22] describes a set of schemes that allow to obtain IA precoders and decoders for downlink MIMO HetNets with partial connectivity. As another example, the feasibility of interference alignment for reverse time division duplex (R-TDD) MIMO two-cell systems is analyzed in [23].

Despite its broad scope, existing theoretical results for

This work has been supported by the Ministerio de Economía y Competitividad (MINECO) of Spain, under grants TEC2013-47141-C4-R (RACHEL), TEC2016-75067-C4-4-R (CARMEN), MTM2014-57590-P, and FPI grant BES-2014-069786.

Jacobo Fanjul, Óscar González and Ignacio Santamaria are with the Department of Communications Engineering, University of Cantabria, 39005 Santander, Spain (e-mail: fanjulj@unican.es; oscar.gonzalezf@alumnos.unican.es; i.santamaria@unican.es).

Carlos Beltrán is with the Departamento de Matemáticas, Estadística y Computación, Universidad de Cantabria, 39005 Santander, Spain (e-mail: beltranc@unican.es).

Parts of this work have been presented in [1].

The results presented in this work are reproducible. The Matlab code and datasets are available at https://gtas.unican.es/homotopyIATSP

X networks are also scarce, most of them focusing on the 2-user X channel. In particular, the total number of DoF when both users are equipped with the same number of antennas (symmetric 2-user X channel), along with an outer bound for the asymmetric case, were obtained in [2]. Recently, the authors in [24] proposed a scheme achieving the aforementioned bound. A DoF bound for the $M \times N$-user X network when all nodes are equipped with the same number of antennas and have symmetric message demands was proposed and shown to be achievable in [25] and [26], respectively. In the case of asymmetric demands, the results in [27] apply. Finally, [26] extended the *properness* condition in [28] to provide an upper bound on the linear DoF without channel extensions, although the tightness of the proposed bound was not analyzed.

A few algorithms for computing IA solutions have also been proposed for the 2-user X channel. First, Jafar and Shamai [2] proposed the so-called JS-scheme for the 2-user MIMO X channel, which is able to achieve the outer bound for some antenna configurations. Later, Agustín and Vidal [24], [29] presented an algorithm based on the generalized singular value decomposition that attains the outer DoF bound for any antenna configuration including channel or symbol extensions. However, these algorithms are again limited to the 2-user X channel and are not easily generalizable to arbitrary X networks. Similarly, IA algorithms originally developed for other topologies (IC, IMAC or IBC) cannot be straightforwardly adapted to X networks. The reason for this is that in the X network every link acts as both a desired and an interfering link and, due to this coupling, these algorithms are not able to guarantee the rank of the signal in the desired links at the same time they null out the interference.

A. Summary of Contributions

In this paper we propose an algorithm, which extends and generalizes our previous work in [1], to compute interference alignment solutions for general asymmetric X networks. It is based on homotopy continuation, a numerical method which is frequently used to solve multivariate systems of nonlinear equations [30]–[33]. More specifically, the main contributions are as follows:

- In comparison to [1], which was proposed only for generic channels, in this work we explicitly enforce the rank constraints on the direct channels by representing them as an additional set of bilinear equations. In this way, the new algorithm is able to find alignment precoders and decoders also in scenarios with symbol extensions, which result in non-generic (structured) MIMO channels. Also, the additional set of rank conditions allows to apply this method to rank-deficient channels, such as the ones studied in [34], [35].
- We describe a simple procedure to obtain a start system for the homotopy continuation method.
- We prove that for many feasible systems and for a sufficiently small step size in the prediction and correction steps, the homotopy continuation algorithm converges to an IA solution for the target system with probability one.
- We show that the proposed algorithm can be applied to a large number of scenarios ranging from conventional network topologies such as the IC, IMAC or IBC [5]–[7], [11], [12], [14]–[17], [20], to new scenarios that appear in the context of HetNets [21]–[23] such as reverse TDD systems, with or without symbol extensions.
- By means of Monte Carlo simulations, we show that the proposed algorithm clearly outperforms alternating minimization-based algorithms in terms of achieved DoF, and it is able to find the maximum DoF IA solution with high success probability[1].

B. Paper Organization

This paper is organized as follows. In Section II we present the general X network system model. In Section III, the proposed algorithm is described in detail, including several implementation details within Section III-C. Section IV is dedicated to the theoretical convergence analysis of the homotopy continuation method. In Section V, we study some well-known network topologies as particular cases of X networks. In Section VI the homotopy continuation method is compared to other existing IA algorithms in terms of DoF performance for different network topologies. Finally, we summarize the main conclusions of this work in Section VII.

C. Notation

Uppercase (lowercase) boldface letters will be used for matrices (column vectors); $(\cdot)^H$ for conjugate transpose (Hermitian) and $(\cdot)^+$ for the Moore-Penrose pseudoinverse. $\otimes$ denotes the Kronecker product and $\mathbf{I}_{m,n}$ and $\mathbf{0}_{m,n}$ the $m \times n$ identity and zero matrices, respectively. $\{\mathbf{V}_k\}\ \forall k \in \{1, \ldots, K\}$ will be used to denote a collection of K matrices (precoders, decoders or channel matrices, for instance). Following the definition in [36], the Jacobian of a matrix function $\mathbf{G}(\mathbf{A})$ at $\mathbf{A}$ will be denoted as $D\mathbf{G}(\mathbf{A})$, and we will write an increment in variable $\mathbf{A}$ as $\Delta\mathbf{A}$. Further, we use $\operatorname{vec}\mathbf{A}$ to represent the column-wise vectorization of a matrix $\mathbf{A}$, and we define the operator

$$\operatorname*{cat}_{s}(\mathbf{A}_s)$$

as the horizontal concatenation of the indexed matrices $\mathbf{A}_s$ where the members s of the set S are taken in reflected lexicographic order. For instance, consider the set of tuples $\mathcal{S} = \{(1,2),(2,2),(1,1),(2,1)\}$; then

$$\operatorname*{cat}_{s}(\mathbf{A}_s) = \begin{bmatrix} \mathbf{A}_{1,1} & \mathbf{A}_{2,1} & \mathbf{A}_{1,2} & \mathbf{A}_{2,2} \end{bmatrix}.$$

Let $d_{k\ell}$ denote the elements of a matrix $\mathbf{D}$. Occasionally, we write some elements of $\mathbf{D}$ in a more compact way in order to facilitate a clean reading, hence defining the following equivalence:

$$\mathbf{d}_{k,i:j} = \begin{bmatrix} d_{k,i} & d_{k,i+1} & \cdots & d_{k,j} \end{bmatrix}.$$

[1]Even though the DoF are known to be an appropriate figure of merit only for high signal-to-noise ratio (SNR) regimes, they provide the number of interference-free data streams that can be transmitted in a given scenario and therefore they are of fundamental importance to analyze the performance of any IA algorithm.

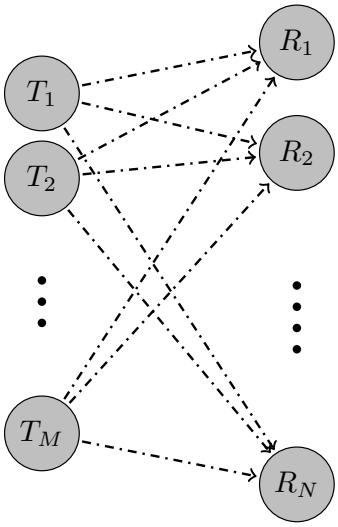

Fig. 1. General MIMO X network model. Dash-dotted lines indicate that both desired signal and interference coexist in the corresponding link.

Similarly, a vector $\mathbf{d}_{i:j,k}$ will have an analogous structure, but as a column vector. Additionally, $\mathbf{D}_{k:\ell,i:j}$ represents a submatrix of $\mathbf{D}$ consisting of the elements in rows k to ℓ and columns i to j.

II. System Model

A. X Network

An $M \times N$ user MIMO X network is a single-hop communication network with M transmitters and N receivers, where transmitter ℓ and receiver k are equipped with A_ℓ and B_k antennas, respectively. Let us introduce the *demands matrix*, $\mathbf{D}$, defined as follows:

$$\mathbf{D} = \begin{bmatrix} d_{11} & d_{12} & \cdots & & d_{1M} \\ d_{21} & \ddots & & & \\ \vdots & & d_{k\ell} & & \vdots \\ & & & \ddots & \\ d_{N1} & & \cdots & & d_{NM} \end{bmatrix},$$

where $d_{k\ell}$ determines the number of independent data streams that transmitter ℓ wishes to send to receiver k, where $\ell \in \{1, 2, \ldots, M\}$, $k \in \{1, 2, \ldots, N\}$. This setting is depicted in Figure 1, where dash-dotted lines indicate that both desired signal and interference coexist in the corresponding link.

Let $\mathbf{V}_{j\ell} \in \mathbb{C}^{A_\ell \times d_{j\ell}}$ be the precoding matrix used by transmitter ℓ to send its $d_{j\ell}$ independent data streams to receiver j. At the other side of the link, receiver k applies a decoding matrix $\mathbf{U}_k \in \mathbb{C}^{B_k \times d_k^{\mathrm{Rx}}}$, where $d_k^{\mathrm{Rx}} = \sum_\ell d_{k\ell}$ is the total number of streams that receiver k wants to decode. Thus, the signal after decoding at the k-th receiver can be expressed as

$$\mathbf{r}_k = \mathbf{U}_k^H \left(\sum_\ell \mathbf{H}_{k\ell}\mathbf{V}_{k\ell}\mathbf{s}_{k\ell} + \sum_\ell \sum_{j \neq k} \mathbf{H}_{k\ell}\mathbf{V}_{j\ell}\mathbf{s}_{j\ell} + \mathbf{n}_k \right), \tag{1}$$

where $\mathbf{s}_{k\ell} \in \mathbb{C}^{d_{k\ell}}$ contains the information that transmitter ℓ is sending to receiver k, $\mathbf{H}_{k\ell} \in \mathbb{C}^{B_k \times A_\ell}$ is the flat-fading MIMO channel from transmitter ℓ to receiver k and $\mathbf{n}_k \in \mathbb{C}^{B_k}$ is the additive and spatially white Gaussian noise at receiver k.

B. IA Conditions

As we have previously mentioned, the key idea of interference alignment consists of designing precoding matrices to reduce the dimension of the interference subspace. In this way, the interference can be zero-forced by the decoders at the corresponding receivers, but at the same time the desired signals at each receiver should be linearly independent. More formally, solving the IA problem amounts to finding a set of precoders and decoders satisfying the following conditions:

$$\mathbf{U}_k^H \mathbf{H}_{k\ell} \mathbf{V}_{\overline{k\ell}} = \mathbf{0}, \quad \forall k, \ell \tag{2}$$

$$\operatorname{rank}\left(\mathbf{U}_k^H \begin{bmatrix} \mathbf{H}_{k1}\mathbf{V}_{k1} & \cdots & \mathbf{H}_{kM}\mathbf{V}_{kM} \end{bmatrix}\right) = d_k^{\mathrm{Rx}}, \quad \forall k, \tag{3}$$

where $\mathbf{V}_{\overline{k\ell}}$ represents the horizontal concatenation of all $\mathbf{V}_{j\ell}$ such that $j \neq k$, i.e.,

$$\mathbf{V}_{\overline{k\ell}} \stackrel{\text{def}}{=} \underset{j \neq k}{\mathrm{cat}}\left(\mathbf{V}_{j\ell}\right).$$

Notice that $\mathbf{U}_k^H \begin{bmatrix} \mathbf{H}_{k1}\mathbf{V}_{k1} & \cdots & \mathbf{H}_{kM}\mathbf{V}_{kM} \end{bmatrix}$ in (3) is a $d_k^{\mathrm{Rx}} \times d_k^{\mathrm{Rx}}$ matrix formed by the concatenation of all equivalent channels (after precoding and decoding) for the k-th user. Condition (2) guarantees that all interferences are properly zero-forced, while (3) preserves the desired signal dimensionality at the intended receivers.

In order to provide some insight into the necessary conditions for the feasibility of the IA problem, we follow the usual approach in the literature [26], [28]. Note that, given the sets of precoders and decoders, $\{\mathbf{V}_{j\ell}\}$ and $\{\mathbf{U}_k\}$, satisfying (2), we can right-multiply them by arbitrary invertible matrices and (2) still holds. Therefore, a total of $d_{k\ell}^2$ ($(d_k^{\mathrm{Rx}})^2$) elements can be arbitrarily fixed in each precoder (decoder) leaving a total of

$$N_v = \sum_{k=1}^{N} \sum_{\ell=1}^{M} \left(A_\ell - d_{k\ell}\right) d_{k\ell} + \sum_{k=1}^{N} \left(B_k - d_k^{\mathrm{Rx}}\right) d_k^{\mathrm{Rx}}$$

free variables. The total number of scalar equations in (2) relating those variables is

$$N_e = \sum_{k=1}^{N} d_k^{\mathrm{Rx}} \left(\sum_{j=1, j \neq k}^{N} d_j^{\mathrm{Rx}} \right).$$

Hence, a natural condition for (2) to be solvable is $N_e \leq N_v$. Given an antenna configuration such that $A_\ell = A$, $B_k = B$, $\forall k, \ell$, and assuming symmetric demands, $d_{k\ell} = d$, $\forall k, \ell$, we can obtain a simplified condition, as established in [26]:

$$d \leq \frac{A + B}{MN + 1}. \tag{4}$$

A network that satisfies $N_e \leq N_v$ is said to be *proper* [28]. Although proper systems are not always feasible, it has been proved for different topologies that improper systems are always infeasible [26], [28], [37], [38].

III. Homotopy Continuation for Vector Space IA

In this section we present a general IA algorithm based on homotopy continuation, which can be applied to arbitray MIMO X networks, possibly including symbol extensions. Homotopy continuation is a numerical method for solving systems of nonlinear equations: the basic idea consists of gradually deforming a trivially solvable system or *start* system into the original problem or *target* system [39]–[42]. This is made by defining a parametrized transformation, which is controlled by a continuation parameter. In the particular case of IA, our goal is to start from a system composed of channels, precoders and decoders that trivially satisfy (2) and (3), and then track the IA solution until the desired precoding and decoding matrices for the target channel.

A. Proposed algorithm

In our previous work [1], we proposed a homotopy function based solely on the interference cancellation conditions (2). However, when symbol or channel extensions are used, we have to explicitly enforce the rank conditions (3) as well. To this end, in this work we propose a different homotopy function that reformulates the rank conditions as a new set of bilinear equations which then can be easily combined with the alignment bilinear equations (2). We start by changing (3) to

$$\mathbf{U}_k^H \begin{bmatrix} \mathbf{H}_{k1}\mathbf{V}_{k1} & \cdots & \mathbf{H}_{kM}\mathbf{V}_{kM} \end{bmatrix} = \mathbf{I}_{d_k^{\mathrm{Rx}}}, \quad \forall k. \tag{5}$$

Note that a solution to (2), (5) is a solution of (2), (3), and reciprocally if a solution to (2), (3) is known then a solution to (2), (5) is produced by right–multiplying each precoder by an appropriate invertible square matrix[2]. We can therefore substitute (2), (3) by (2), (5), and in this way the IA problem now amounts to solving an extended set of bilinear equations. In order to include both (2) and (5), this extended set of equations can be written more compactly as follows:

$$\mathbf{U}_k^H \mathbf{H}_{k\ell}\mathbf{V}_{k\ell} = \mathbf{P}_{k\ell} \quad \forall k, \ell, \tag{6}$$

where $\mathbf{P}_{k\ell}$ is a block of $d_{k\ell}$ columns extracted from the $d_k^{\mathrm{Rx}} = \sum_\ell d_{k\ell}$ identity matrix, $\mathbf{I}_{d_k^{\mathrm{Rx}}}$, i.e.,

$$\mathbf{P}_{k\ell} = \begin{bmatrix} \mathbf{e}_{i+1} & \mathbf{e}_{i+2} & \cdots & \mathbf{e}_{i+d_{k\ell}} \end{bmatrix},$$

where $\mathbf{e}_i$ is a column vector with all zero elements except for a 1 in the i-th position, and $i = \sum_{n=1}^{k-1} d_{n\ell}$.

Let $d_\ell^{\mathrm{Tx}} = \sum_k d_{k\ell}$ be the total number of messages that the ℓ-th user wishes to transmit, and let $\mathbf{V}_\ell$ be the horizontal concatenation of all $\mathbf{V}_{j\ell}$,

$$\mathbf{V}_\ell \stackrel{\text{def}}{=} \underset{j}{\mathrm{cat}}\big(\mathbf{V}_{j\ell}\big).$$

With this notation, the alignment equations in (6) can be rewritten as

$$\mathbf{U}_k^H \mathbf{H}_{k\ell}\mathbf{V}_\ell = \mathbf{A}_{k\ell} \quad \forall k, \ell, \tag{7}$$

[2]This trick is used later in (13) to obtain a start system for the homotopy continuation method. Notice that the decoders obtained this way are not necessarily given by matrices with orthogonal columns.

where, again, $\mathbf{U}_k \in \mathbb{C}^{B_k \times d_k^{\mathrm{Rx}}}$ is the decoding matrix for receiver k, $\mathbf{H}_{k\ell} \in \mathbb{C}^{B_k \times A_\ell}$ is the flat-fading MIMO channel from transmitter ℓ to receiver k, and $\mathbf{V}_\ell \in \mathbb{C}^{A_\ell \times d_\ell^{\mathrm{Tx}}}$ is the precoding matrix applied by transmitter ℓ. Additionally, $\mathbf{A}_{k\ell} = \begin{bmatrix} \mathbf{0} & \cdots & \mathbf{P}_{k\ell} & \cdots & \mathbf{0} \end{bmatrix}$ is a $d_k^{\mathrm{Rx}} \times d_\ell^{\mathrm{Tx}}$ matrix such that $\mathbf{P}_{k\ell}$ is the only block in $\mathbf{A}_{k\ell}$ containing non-zero elements. Therefore, $\mathbf{A}_{k\ell}$ includes all interference cancellation and rank preservation equations related to channel $\mathbf{H}_{k\ell}$.

According to these compacted bilinear equations, we define the function that will allow us to obtain the precoders, $\mathbf{V}_\ell$, and decoders, $\mathbf{U}_k^H$. Let us first consider a parametrized channel matrix, $\mathbf{H}_{k\ell}(t)$, as a convex combination of a *start* channel, $\overline{\mathbf{H}}_{k\ell}$, and the *target* channel, $\mathbf{H}_{k\ell}$. This combination is controlled by the continuation parameter, t, leading to a homotopy function given by

$$\mathbf{G}_{k\ell}(\mathbf{U}_k^H, \mathbf{V}_\ell, t) = \mathbf{U}_k^H \underbrace{\big((1-t)\overline{\mathbf{H}}_{k\ell} + t\mathbf{H}_{k\ell}\big)}_{\mathbf{H}_{k\ell}(t)} \mathbf{V}_\ell - \mathbf{A}_{k\ell}, \tag{8}$$

$\forall k, \ell$ and $t \in [0, 1]$. Our goal is to move the solution along the path $\mathbf{G}_{k\ell}(\mathbf{U}_k^H, \mathbf{V}_\ell, t) = \mathbf{0}$ $\forall k, \ell$ from $t = 0$ to $t = 1$ in a finite number of steps Δt. Usually, this path tracking procedure is accomplished by an iterative predictor/corrector method [42], which is commonly known as *simple path tracker*. In particular, a first order approximation of the homotopy function in (8), which is given by

$$\begin{aligned} \mathbf{G}_{k\ell}(\mathbf{U}_k^H + \Delta\mathbf{U}_k^H, \mathbf{V}_\ell + \Delta\mathbf{V}_\ell, t + \Delta t) = \\ \mathbf{U}_k^H\mathbf{H}_{k\ell}(t)\mathbf{V}_\ell + \Delta\mathbf{U}_k^H\mathbf{H}_{k\ell}(t)\mathbf{V}_\ell \\ + \mathbf{U}_k^H\mathbf{H}_{k\ell}(t)\Delta\mathbf{V}_\ell \\ + \mathbf{U}_k^H(\mathbf{H}_{k\ell} - \overline{\mathbf{H}}_{k\ell})\mathbf{V}_\ell\Delta t - \mathbf{A}_{k\ell}, \quad \forall k, \ell \end{aligned} \tag{9}$$

gives rise to the basic Euler prediction and Newton correction steps. Assuming that there is a point $(\{\mathbf{U}_k^H\}, \{\mathbf{V}_\ell\}, t)$ close enough to the path (i.e., $\mathbf{U}_k^H\mathbf{H}_{k\ell}(t)\mathbf{V}_\ell \approx \mathbf{A}_{k\ell}$ $\forall k, \ell$), we may predict an approximate solution at $t + \Delta t$ by setting $\mathbf{G}_{k\ell}(\mathbf{U}_k^H + \Delta\mathbf{U}_k^H, \mathbf{V}_\ell + \Delta\mathbf{V}_\ell, t + \Delta t) = \mathbf{0}$:

$$\begin{aligned} \Delta\mathbf{U}_k^H\mathbf{H}_{k\ell}(t)\mathbf{V}_\ell + \mathbf{U}_k^H\mathbf{H}_{k\ell}(t)\Delta\mathbf{V}_\ell = \\ -\mathbf{U}_k^H(\mathbf{H}_{k\ell} - \overline{\mathbf{H}}_{k\ell})\mathbf{V}_\ell\Delta t \quad \forall k, \ell. \end{aligned} \tag{10}$$

Updates $\Delta\mathbf{V}_\ell$ and $\Delta\mathbf{U}_k^H$ $\forall k, \ell$ are obtained by solving –if possible– the system of linear equations in (10). Further details on this point are relegated to Subsection III-C.

Additionally, if the current point $(\{\mathbf{U}_k^H\}, \{\mathbf{V}_\ell\}, t)$ is not as close to the path as required, i.e., the elements in $\mathbf{G}_{k\ell}(\mathbf{U}_k^H, \mathbf{V}_\ell, t)$ are greater than a predefined tolerance, we may hold t constant by setting $\Delta t = 0$ and obtain the Newton correction step:

$$\begin{aligned} \Delta\mathbf{U}_k^H\mathbf{H}_{k\ell}(t)\mathbf{V}_\ell + \mathbf{U}_k^H\mathbf{H}_{k\ell}(t)\Delta\mathbf{V}_\ell = \\ \mathbf{A}_{k\ell} - \mathbf{U}_k^H\mathbf{H}_{k\ell}(t)\mathbf{V}_\ell, \ \forall k, \ell. \end{aligned} \tag{11}$$

Analogously to the prediction procedure, precoder and decoder updates, $\Delta\mathbf{V}_\ell$ and $\Delta\mathbf{U}_k^H$ $\forall k, \ell$, are calculated by solving –if possible– the system of linear equations in (11).

This step leads to a new set of precoding and decoding matrices, $\{\mathbf{V}_\ell+\Delta\mathbf{V}_\ell\}$ and $\{\mathbf{U}_k^H+\Delta\mathbf{U}_k^H\}$, which are expected to lie closer to the tracked path.

B. Start system

As we have already mentioned, one important step in homotopy continuation methods is the choice of a start system composed of a set of precoders $\left\{\overline{\mathbf{V}}_\ell\right\}$, decoders $\left\{\overline{\mathbf{U}}_k\right\}$ and channels $\left\{\overline{\mathbf{H}}_{k\ell}\right\}$, which satisfies (7) and that it is easy to compute.

A first idea is to look at (7) as if we were given $\left\{\overline{\mathbf{U}}_k\right\}$ and $\left\{\overline{\mathbf{V}}_\ell\right\}$ (for instance, we might use randomly generated precoders and decoders) and we had to solve it for $\left\{\overline{\mathbf{H}}_{k\ell}\right\}$. This is naturally called the inverse IA problem in [38], and it is an easily solvable linear problem for some network topologies such as the MIMO-IC without symbol extensions. However, for general MIMO X networks it is unlikely that a randomly chosen collection of precoders and decoders will satisfy (7) for *some* channel. The three objects (channel, precoders and decoders) must be chosen simultaneously. To this end, in this paper we propose an alternative procedure that first obtains a start system composed of precoders, decoders and channels satisfying the zero-forcing alignment conditions (2), and then modifies this start system to fulfill the extended set of equations in (7).

First, we randomly generate a set of precoders and decoders; second, we obtain the channels as follows

$$\overline{\mathbf{H}}_{k\ell} = \mathbf{X}_{k\ell} - \mathbf{F}_k\mathbf{F}_k^H\mathbf{X}_{k\ell}\mathbf{C}_{\overline{k\ell}}\mathbf{C}_{\overline{k\ell}}^H, \quad \forall k,\ell \tag{12}$$

where $\mathbf{F}_k$ and $\mathbf{C}_{\overline{k\ell}}$ are orthonormal bases of $\overline{\mathbf{U}}_k$ and $\overline{\mathbf{V}}_{\overline{k\ell}}$, respectively, and $\mathbf{X}_{k\ell}$ is a non-zero arbitrary random matrix. Notice that by calculating $\overline{\mathbf{H}}_{k\ell}$ as in (12), the interference cancellation conditions (2) are trivially satisfied. Now, as mentioned in Section II, we can right-multiply either the precoders or the decoders by arbitrary invertible matrices and (2) still holds. Therefore, by applying the transformation

$$\overline{\mathbf{U}}_k' = \overline{\mathbf{U}}_k\left(\left(\overline{\mathbf{U}}_k^H\left[\begin{array}{ccc}\overline{\mathbf{H}}_{k1}\overline{\mathbf{V}}_{k1} & \cdots & \overline{\mathbf{H}}_{kM}\overline{\mathbf{V}}_{kM}\end{array}\right]\right)^H\right)^{-1}, \quad \forall k, \tag{13}$$

(if the inverse exists) the new system comprised of the sets $\left\{\overline{\mathbf{V}}_{k\ell}\right\}$, $\left\{\overline{\mathbf{U}}_k'\right\}$ and $\left\{\overline{\mathbf{H}}_{k\ell}\right\}$ satisfies (2) and (5), and thus (7). We can then use it as a start system for the homotopy continuation procedure.

C. Implementation details

In this section, we discuss some important implementation aspects of the proposed algorithm.

The expressions for the Euler prediction and Newton correction steps are given by (10) and (11), respectively. Now, in order to simplify the algorithm implementation, it is convenient to define a new vector $\mathbf{w} = \left[\underset{\ell}{\mathrm{cat}}((\mathrm{vec}\,\mathbf{V}_\ell)^T), \underset{k}{\mathrm{cat}}((\mathrm{vec}\,\mathbf{U}_k^H)^T)\right]^T$ by stacking all precoding and decoding matrices. Both (10) and (11) represent systems of linear equations which can be conveniently solved as large sparse linear systems. Starting with the prediction step, our goal is to write the set of linear equations in (10) as a single linear equation, $D\mathbf{G}\left(\mathbf{w}\right)\Delta\mathbf{w} = -D\mathbf{G}\left(t\right)$. Applying the identity

$$\mathrm{vec}(\mathbf{ABC}) = \left(\mathbf{C}^T\otimes\mathbf{A}\right)\mathrm{vec}(\mathbf{B}), \tag{14}$$

we first vectorize (10) as

$$\begin{aligned}&\underbrace{\left(\left(\mathbf{V}_\ell^T\mathbf{H}_{k\ell}^T(t)\right)\otimes\mathbf{I}_{d_k^{Rx}}\right)}_{D\mathbf{G}_{k\ell}(\mathbf{U}_k^H)}\Delta\mathrm{vec}\,\mathbf{U}_k^H\\ &+\underbrace{\left(\mathbf{I}_{d_\ell^{Tx}}\otimes\left(\mathbf{U}_k^H\mathbf{H}_{k\ell}(t)\right)\right)}_{D\mathbf{G}_{k\ell}(\mathbf{V}_\ell)}\Delta\mathrm{vec}\,\mathbf{V}_\ell\\ &=-\underbrace{\mathrm{vec}\left(\mathbf{U}_k^H(\mathbf{H}_{k\ell}-\overline{\mathbf{H}}_{k\ell})\mathbf{V}_\ell\right)}_{D\mathbf{G}_{k\ell}(t)}\Delta t, \quad \forall k,\ell.\end{aligned} \tag{15}$$

Once the equations have been vectorized, we can stack them together to represent the Euler prediction step:

$$D\mathbf{G}(\mathbf{w})\Delta\mathbf{w} = -D\mathbf{G}(t)\Delta t \;\Rightarrow\; \Delta\mathbf{w} = -D\mathbf{G}(\mathbf{w})^+D\mathbf{G}(t)\Delta t, \tag{16}$$

where $D\mathbf{G}\left(\mathbf{w}\right)$ is the Jacobian matrix of the system of matrix equations in (7), comprising all the derivatives with respect to the variables $\{\mathbf{V}_{j\ell}\}$ and $\{\mathbf{U}_k^H\}$ in the order specified in (19). It is a block partitioned matrix with as many row partitions as channel matrices and as many column partitions as precoding and decoding matrices. Sparsity comes from the fact that each equation involves a subset of the variables and, therefore, many blocks in (19) are zero. Specifically, $D\mathbf{G}_{k\ell}\left(\mathbf{V}_{jp}\right) = \mathbf{0}$ when $p\neq\ell$, and $D\mathbf{G}_{k\ell}\left(\mathbf{U}_j^H\right) = \mathbf{0}$ when $j\neq k$. The solution vector $\Delta\mathbf{w}$ contains the updates for all the variables in both precoders and decoders, and the derivate with respect to the continuation parameter is built from all partial derivatives as $D\mathbf{G}\left(t\right) = \underset{(k,\ell)}{\mathrm{cat}}\left(D\mathbf{G}_{k\ell}\left(t\right)^T\right)^T$.

Following the same steps, the Newton correction expressions can be rewritten as the solution of a linear equation, $D\mathbf{G}\left(t\right)\Delta w = \mathbf{g}$, obtained by vectorizing all the equations in (11),

$$\begin{aligned}&D\mathbf{G}_{k\ell}(\mathbf{U}_k^H)\Delta\mathrm{vec}\,\mathbf{U}_k^H + D\mathbf{G}_{k\ell}(\mathbf{V}_\ell)\Delta\mathrm{vec}\,\mathbf{V}_\ell\\ &\quad=\underbrace{\mathrm{vec}\left(\mathbf{A}_{k\ell}-\mathbf{U}_k^H\mathbf{H}_{k\ell}(t)\mathbf{V}_\ell\right)}_{\mathbf{g}_{k\ell}}, \quad \forall k,\ell,\end{aligned} \tag{17}$$

and then stacking up all the equations together,

$$D\mathbf{G}(\mathbf{w})\Delta\mathbf{w} = \mathbf{g} \;\Rightarrow\; \Delta\mathbf{w} = D\mathbf{G}(\mathbf{w})^+\mathbf{g}, \tag{18}$$

where $\mathbf{g} = \underset{k,\ell}{\mathrm{cat}}(\mathbf{g}_{k\ell}^T)^T$.

Theoretically, the Newton step should be executed iteratively for a fixed t until a point below the predefined tolerance has been obtained. Since the Newton method converges quadratically to a point in the path, a common strategy is to run the correction step a few times establishing a limit on the number of executions to a maximum of `MaxNwtIter` or until all the entries of $\mathbf{g}$ are below a predefined tolerance `NwtTol`, whatever happens first. Nevertheless, in those cases in which the step size, Δt, is too large, the precoders and

$$D\mathbf{G}(\mathbf{w}) = \left[\begin{array}{cccc|ccc} D\mathbf{G}_{11}(\mathbf{V}_{11}) & D\mathbf{G}_{11}(\mathbf{V}_{21}) & \cdots & D\mathbf{G}_{11}(\mathbf{V}_{NM}) & D\mathbf{G}_{11}(\mathbf{U}_1^H) & \cdots & D\mathbf{G}_{11}(\mathbf{U}_N^H) \\ D\mathbf{G}_{21}(\mathbf{V}_{11}) & & & & & & \\ \vdots & & D\mathbf{G}_{k\ell}(\mathbf{V}_{jp}) & \vdots & \vdots & D\mathbf{G}_{k\ell}(\mathbf{U}_j^H) & \vdots \\ D\mathbf{G}_{NM}(\mathbf{V}_{11}) & \cdots & & D\mathbf{G}_{NM}(\mathbf{V}_{NM}) & D\mathbf{G}_{NM}(\mathbf{U}_1^H) & \cdots & D\mathbf{G}_{NM}(\mathbf{U}_N^H) \end{array}\right] \tag{19}$$

Algorithm 1: Interference alignment via homotopy continuation in MIMO X networks.

Input: $\{\mathbf{H}_{k\ell}\}$, Δt, `NwtTol`, `MaxNwtIter`, `MinStepSize`, `NumHitsToDoubleStep`
Output: $\{\mathbf{V}_\ell\}$ and $\{\mathbf{U}_k\}$ satisfying (2) and (3), and a convergence indicator, PathFailed

`/* Inverse IA */`
Obtain $\left\{\overline{\mathbf{V}}_{k\ell}\right\}$, $\left\{\overline{\mathbf{U}}'_k\right\}$, $\{\overline{\mathbf{H}}_{k\ell}\}$ as shown in (12), (13);
$t = 0$, NumHits $= 0$, PathFailed $=$ `false`
$\mathbf{w} = \left[\underset{(\ell)}{\text{cat}}((\text{vec}\,\mathbf{V}_\ell)^T), \underset{k}{\text{cat}}((\text{vec}\,\mathbf{U}_k^H)^T)\right]^T$
$t^* = t$, $\mathbf{w}^* = \mathbf{w}$ `// backup variables`
while $t < 1$ **do**
  $t = \min(t + \Delta t, 1)$
  `/* Euler prediction */`
  $\mathbf{w} = \mathbf{w} - D\mathbf{G}(\mathbf{w})^+ D\mathbf{G}(t)\Delta t$ as indicated in (16)
  `/* Newton correction */`
  NewtonFailed $=$ `true`
  for *iter* $= 1$ **to** *MaxNwtIter* **do**
    $\mathbf{w} = \mathbf{w} + D\mathbf{G}(\mathbf{w})^+\mathbf{g}$ as shown in (18)
    if $||\mathbf{g}||^2 <$ *NwtTol* **then**
      NumHits $=$ NumHits $+ 1$
      NewtonFailed $=$ `false`
      break
  `/* Step size adaptation routine */`
  if *NumHits* $==$ *NumHitsToDoubleStep* **then**
    $\Delta t = 2\Delta t$
    $t^* = t$, $\mathbf{w}^* = \mathbf{w}$, NumHits $= 0$
  else if *NewtonFailed* **then**
    $\Delta t = \Delta t/2$
    $t = t^*$, $\mathbf{w} = \mathbf{w}^*$, NumHits $= 0$
    if $\Delta t <$ *MinStepSize* **then**
      PathFailed $=$ `true`
      return
Find orthonormal basis for the precoders and decoders satisfying $\mathbf{V}_{k\ell}^H\mathbf{V}_{k\ell} = \mathbf{I}$, $\mathbf{U}_k^H\mathbf{U}_k = \mathbf{I}$, $\quad\forall k, \ell$
return

decoders after the Euler prediction might be so far from the path that the Newton correction step could require several iterations to reach the tolerance value, or it might escape from the basin of attraction of Newton's operator and thus be unable to follow the correct path. In this sense, although there is theoretical evidence proving that there is always a step size, Δt, small enough to assure convergence [41], a fixed step size strategy might not be efficient in practice.

To deal with this issue, we have provided the simple path tracker with an additional feature, allowing our algorithm to adapt the continuation step size depending on the Newton corrector success or failure. A common practice is to halve the step size if we detect that the Euler prediction has failed, and then repeat it. If a number of repeated failed predictions is obtained –i.e. if the step size becomes smaller than a predefined minimum step size, `MinStepSize`– we stop the path tracking procedure and no output is produced. Conversely, if the correction step is successful for `NumHitsToDoubleStep` consecutive iterations, we can double the step size in order to reduce the total number of iterations of the path tracking routine. Algorithm 1 describes the proposed method in full detail[3]. Let us finally remind the reader that a Matlab implementation of this algorithm is available at https://gtas.unican.es/homotopyIATSP.

IV. Convergence analysis

In this section, we analyze the convergence of the homotopy continuation method and provide some important details regarding the implementation of the algorithm.

Let us define the two following spaces:

$$\mathcal{I} = \{(\mathbf{H}_{k\ell}) : \ell \in \{1, \ldots, M\}, k \in \{1, \ldots, N\}\},$$
$$\mathcal{O} = \{(\mathbf{U}_k, \mathbf{V}_{j\ell}) : \ell \in \{1, \ldots, M\}, j, k \in \{1, \ldots, N\}\},$$

which can be thought of as the space of possible "inputs" (channel matrices) and the set of possible "outputs" (precoders and decoders) of the algorithm. Note that an element of $\mathcal{I}$ or $\mathcal{O}$ is just a concatenation of complex matrices. We assume that the order of such concatenation is fixed and we can thus identify

$$\mathcal{I} \equiv \mathbb{C}^a, \quad \mathcal{O} \equiv \mathbb{C}^b,$$

where

$$a = \sum_{k,\ell} A_\ell B_k, \quad b = \sum_k B_k d_k^{\text{Rx}} + \sum_\ell A_\ell d_\ell^{Tx}.$$

Note that alternatively to (7) we can consider the same equations but changing Hermitian transpose to transpose:

$$\mathbf{U}_k^T\mathbf{H}_{k\ell}\mathbf{V}_\ell = \mathbf{A}_{k\ell} \quad \forall k, \ell. \tag{20}$$

Mathematically, it is more simple to deal with this case since the functions involved are then (complex) analytic, so we

[3]For our actual implementation of the proposed method, the input parameters of the algorithm take the following values: $\Delta t = 10^{-3}$, `NwtTol` $= 10^{-10}$, `MaxNwtIter` $= 5$, `MinStepSize` $= 10^{-15}$ and `NumHitsToDoubleStep` $= 3$

consider these equivalent equations in this section. Obviously, a solution to (20) produces and answer to (7) and viceversa, so there is no harm in this change. In the rest of this section, we will focus on the most challenging case that happens when the solution set for any given $\mathbf{H} = (\mathbf{H}_{k\ell}) \in \mathcal{I}$ (out of some zero–measure set) is finite [43]. In words, this is the situation of a tightly-feasible scenario in which removing a single antenna at any transmitter or receiver turns the system unfeasible [44].

Recall that, for fixed $\mathbf{H} \in \mathcal{I}$, a point $(\mathbf{U}_k, \mathbf{V}_{j\ell}) \in \mathcal{O}$ is a *nonsingular* solution of (20) if the linear mapping given by the derivative:

$$(\dot{\mathbf{U}}_k, \dot{\mathbf{V}}_{k\ell}) \to \dot{\mathbf{U}}_k^T \mathbf{H}_{k\ell}(t)\mathbf{V}_\ell + \mathbf{U}_k^T \mathbf{H}_{k\ell}(t)\dot{\mathbf{V}}_\ell \quad \forall k, \ell \quad (21)$$

is invertible. It is thus easy to check if a solution of (20) is nonsingular (up to numerical errors).

We now state our convergence result

Theorem 1: Let $\overline{\mathbf{H}} \in \mathcal{I}$ and let $(\overline{\mathbf{U}}_k, \overline{\mathbf{V}}_{j\ell})$ be a nonsingular solution of

$$\overline{\mathbf{U}}_k^T \overline{\mathbf{H}}_{k\ell} \overline{\mathbf{V}}_\ell = \mathbf{A}_{k\ell} \quad \forall k, \ell. \quad (22)$$

Then, for almost all $\mathbf{H} \in \mathcal{I}$, the solution $(\overline{\mathbf{U}}_k, \overline{\mathbf{V}}_{j\ell})$ can be smoothly continued using the homotopy $\mathbf{H}(t) = (1-t)\overline{\mathbf{H}} + t\mathbf{H}$ to a nonsingular solution of (20).

Proof: See Appendix A. ∎

In general, we cannot guarantee in advance that the start system in Section III-B satisfies the nonsingularity hypothesis of Theorem 1. However, as pointed out above, checking whether it satisfies the hypothesis is an elementary task, which implies that there are two possibilities regarding the starting pair described in Section III-B:

1) Case 1: our starting alignment solution $(\overline{\mathbf{U}}_k, \overline{\mathbf{V}}_{j\ell})$ defines a nonsingular solution of (22). Then, with probability 1 a channel $\mathbf{H} \in \mathcal{I}$ admits at least one nonsingular alignment solution and we can consider the problem as feasible. Moreover, we can construct a solution for almost all possible inputs by continuing the known one.
2) Case 2: our starting alignment solution $(\overline{\mathbf{U}}_k, \overline{\mathbf{V}}_{j\ell})$ defines a singular solution of (22). In this case, the derivative (21) is singular and hence we cannot continue the solution to the target system using the generated start system. Although the singularity of (21) does not determine if the problem is feasible or unfeasible, in this work we assume that the networks under study are feasible systems. Therefore, it may suffice to perform the procedure in Section III-B again in order to generate a new start system which might define a nonsingular solution of (22) (see Case 1).

Therefore, in the worst scenario we may just have to discard the start system after a simple linear algebra test, and then generate a new starting point as described in Section III-B. This contrasts with other iterative methods such as Alternating Minimization or simply applying Newton's method where one must make a (possibly very long) number of iterations on an initial guess with no a priori guarantee on the convergence of the method.

Of course, the algorithm being a numerical method, there is a chance that, even knowing that a continuation exists, it cannot be found in reasonable time or the homotopy step is too small to be used in practice, see the discussion in Section III-C. Theorem 1 gives however a strong theoretical support to the use of homotopy techniques for the problem under study.

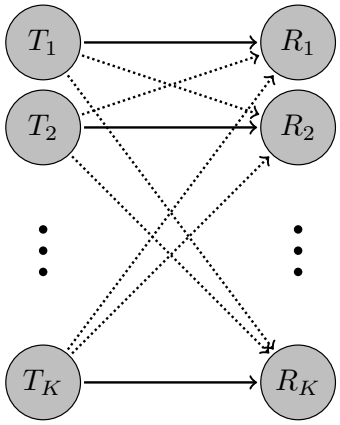

Fig. 2. Interference channel. Solid line arrows represent desired information, and dashed line arrows are associated to interference.

V. Application to common network topologies

As we mentioned in Section I, many well-known network topologies can be viewed as particular cases of the general X network considered in this paper. To make this point clear, in this section we specialize the general X network to IC, IMAC and IBC topologies.

A. Interference channel

An interference channel (cf. Fig. 2) is a particular case of the MIMO X network in which the following conditions are satisfied:

- The number of transmitters is equal to the number of receivers, i.e. $M = N = K$.
- Each transmitter sends its information only to its corresponding receiver. This fact is reflected in the demands matrix, $\mathbf{D}$, by making $d_{k\ell} = 0, \ \forall k \neq \ell$.

Consequently, the alignment conditions (2) and (3) simplify to

$$\mathbf{U}_k^H \mathbf{H}_{k\ell} \mathbf{V}_{\ell\ell} = \mathbf{0}, \quad \forall k, \ \forall \ell \neq k \quad (23)$$

$$\operatorname{rank}\left(\mathbf{U}_k^H \mathbf{H}_{kk} \mathbf{V}_{kk}\right) = d_{kk}, \quad \forall k. \quad (24)$$

Notice that, for generic MIMO interference channels (i.e., without symbol extensions), the rank condition (24) is automatically satisfied as long as both precoders and decoders are full column rank. This is clear by noticing that the channel matrices involved in (24) are independent of those appearing in (23). The alternating minimization algorithm in [6] relies on this fact to solve (23) by restricting the precoding and decoding matrices to lie in the Stiefel manifold, i.e. $\mathbf{V}_{\ell\ell}^H \mathbf{V}_{\ell\ell} = \mathbf{I}$ and $\mathbf{U}_k^H \mathbf{U}_k = \mathbf{I}$.

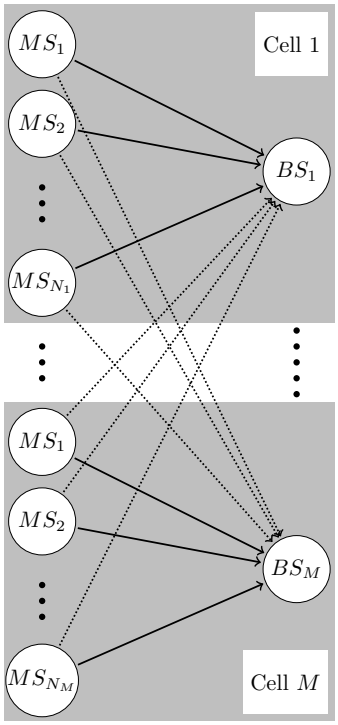

Fig. 3. Interference multiple-access channel. Solid line arrows represent desired information, and dashed line arrows are associated to interference.

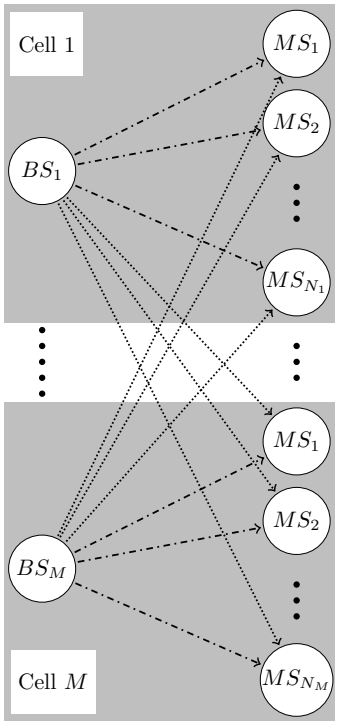

Fig. 4. Interference broadcast channel. Dashed line arrows are associated to interference, and dash-dotted lines indicate that both desired and interfering signals coexist in the same link.

B. Cellular networks

Cellular networks can also be viewed as particular cases of X networks. More specifically, two dual topologies have been traditionally used to characterize both the uplink and downlink channels in cellular systems, namely the interference multiple-access channel (IMAC) and interference broadcast channel (IBC) models, which are depicted in Figs. 3 and 4 respectively. Whereas in traditional cellular systems all cells operate synchronously either in uplink or dowlink mode, in this paper we also consider a heterogeneous network (HetNet) scenario in which some cells may operate in uplink mode while the rest of them operate in downlink. This configuration is known as reverse time division duplex (R-TDD), and it has been shown to increase the number of achievable DoF in some scenarios [23]. An example of an R-TDD, two-cell network is shown in Fig. 5.

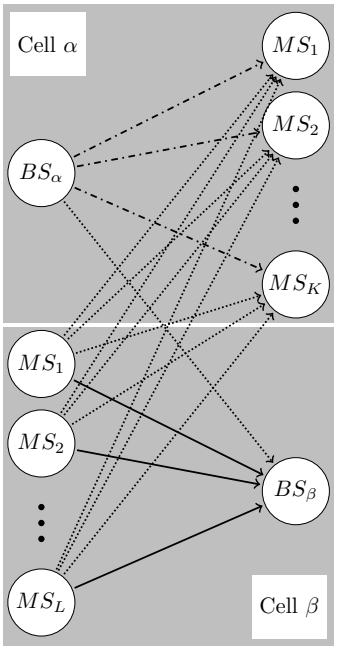

Fig. 5. Reverse TDD model. Solid line arrows represent desired information, and dashed line arrows are associated to interference. Dash-dotted lines indicate that both desired and interfering signals coexist in the same link.

An IMAC, IBC, or reverse TDD cellular network with M cells and $N = \sum_k N_k$ users per cell can be viewed as an X network with the following characteristics.

1) Interference multiple-access channel (IMAC):

- The demands matrix, $\mathbf{D} = \mathbf{D}_{IMAC}$, has a block-diagonal structure, as shown in (25).
- The number of transmitters will be equal to the total number of mobile stations within the network, and the number of receivers will correspond to the number of base stations.

2) Interference broadcast channel (IBC):

- The demands matrix, $\mathbf{D} = \mathbf{D}_{IBC}$, has a block-diagonal structure, as shown in (26).
- The number of transmitters coincides with the number of base stations, and the number of receivers is the number of mobile stations.

3) Reverse TDD:

- Since this type of networks consists of both multiple-access channels and broadcast channels, the demands

$$\mathbf{D}_{IMAC} = \begin{bmatrix} \mathbf{d}_{1,1:N_1} & \mathbf{0}_{1,N_2} & \mathbf{0} & \cdots & \mathbf{0} & \mathbf{0}_{1,N_M} \\ \mathbf{0}_{1,N_1} & \mathbf{d}_{2,N_1+1:N_2} & \mathbf{0} & \cdots & & \mathbf{0}_{1,N_M} \\ & & \ddots & & & \\ \vdots & & \mathbf{0} & \mathbf{d}_{k,\sum_{\ell=1}^{k-1} N_\ell+1:\sum_{\ell=1}^{k} N_\ell} & \mathbf{0} & \vdots \\ & & & & \ddots & \\ \mathbf{0}_{1,N_1} & \mathbf{0}_{1,N_2} & \mathbf{0} & \cdots & \mathbf{0} & \mathbf{d}_{M,N-N_M+1:N} \end{bmatrix} \tag{25}$$

$$\mathbf{D}_{IBC} = \begin{bmatrix} \mathbf{d}_{1:N_1,1} & \mathbf{0}_{N_1,1} & \mathbf{0} & \cdots & \mathbf{0} & \mathbf{0}_{N_1,1} \\ \mathbf{0}_{N_2,1} & \mathbf{d}_{N_1+1:N_2,2} & \mathbf{0} & \cdots & & \mathbf{0}_{N_2,1} \\ & & \ddots & & & \\ \vdots & & \mathbf{0} & \mathbf{d}_{\sum_{\ell=1}^{k-1} N_\ell+1:\sum_{\ell=1}^{k} N_\ell,k} & \mathbf{0} & \vdots \\ & & & & \ddots & \\ \mathbf{0}_{N_M,1} & \mathbf{0}_{N_M,1} & \mathbf{0} & \cdots & \mathbf{0} & \mathbf{d}_{N-N_M+1:N,M} \end{bmatrix} \tag{26}$$

matrix, $\mathbf{D}$, will be a combination of (25) and (26), depending on the particular uplink/downlink configuration.

- The number of transmitters will be the number of downlink base stations plus the uplink mobile stations. The number of receiving nodes will be the sum of base stations in uplink mode and mobile stations in downlink mode.

VI. Simulation Results

In this section we evaluate the performance of the homotopy continuation IA algorithm by means of Monte Carlo simulations in a number of different network topologies. More specifically, the performance of the method is evaluated on the following scenarios:

- A 4-user MIMO X network including three different antenna configurations (Scenarios 1, 2, and 3).
- An interference channel (IC) and a 2-user X channel (Scenarios 4 and 5, respectively), both with symbol extensions.
- An interference multiple-access channel (IMAC) and an interference broadcast channel (IBC).
- Finally, the proposed algorithm will be tested on a reverse time division duplex (R-TDD) scenario. IMAC, IBC and R-TDD settings are evaluated for the same cellular network (Scenario 6).

For each configuration, the results of 1000 independent Rayleigh channel realizations were averaged.

A. 4-user MIMO X network

We consider a 4-user MIMO X network as our first scenario and evaluate the sum-rate performance of the proposed method (denoted as `HC`) in comparison to the minimum interference leakage (`MinIL`) alternating minimization algorithm proposed in [6], which has been conveniently adapted to operate in MIMO X networks.

The comparison scenario is a MIMO X network comprised of $M = 4$ transmitters and $N = 4$ receiver nodes, satisfying $M = N = K$, equipped with A and B antennas, respectively. Each transmitter wishes to send one stream to each receiver, i.e., $d_{k\ell} = d = 1\ \forall k, \ell$. As shown in Table I, three different antenna configurations were simulated. Notice that the bound in (4) holds with equality for Scenario 1, which has the minimum number of antennas to ensure feasibility.

Although there exists numerical evidence that for feasible systems the `MinIL` method always converges to the global minimum for generic interference channels, it does not guarantee the rank conditions in (3) for an X network. This is due to the fact that, as it was mentioned before, in an X network every link acts as both a desired and an interfering link. Since the proposed algorithm takes both interference cancellation and rank preservation conditions into account, it clearly outperforms the results achieved by `MinIL` in terms of degrees of freedom, especially in the tightest scenarios, as Fig. 6 shows. Note that the sum-rate slope in the high signal-to-noise-ratio (SNR) regime attained by `HC` in Scenario 1 is even higher than that achieved by `MinIL` in Scenario 3, with the advantage of `HC` using fewer antennas than `MinIL`. As the number of antennas is increased, the performance of `MinIL` improves, requiring at least 10 antennas at both ends of the link to obtain the requested DoF.

Of course, the probability of attaining the requested DoF affects the average sum-rate performance. As shown in Table I, we observe that the probability of achieving the maximum of $K^2d = 16$ DoF is significantly higher for the `HC` algorithm, being close to 1 for the 3 considered scenarios. This is in agreement with the theoretical convergence result proved in Theorem 1, and provides strong support for the use of the homotopy continuation algorithm in MIMO X networks.

B. Channel Extensions

In the second example, we evaluate the performance of the HC algorithm when symbols extensions are used. To this end, two different network configurations, namely, an interference channel and a 2-user X channel are considered.

TABLE I
Prob[DoF $= K^2d = 16$] OR PROBABILITY OF ACHIEVING THE REQUESTED NUMBER OF DEGREES OF FREEDOM FOR $K = 4$ AND $d = 1$.

Scenario	1	2	3
$(A, B) =$	$(8, 9)$	$(9, 9)$	$(10, 10)$
HC	0.98	0.99	1.00
MinIL	0.00	0.00	0.44

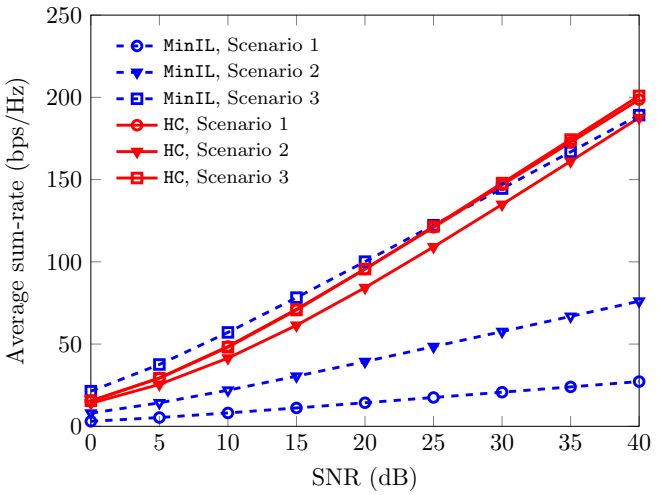

Fig. 6. Average sum-rate achieved by MinIL and HC in the three considered scenarios.

Regarding the IC, the scenario under test is comprised of $K = 6$ users, each transmitter is equipped with $A = 2$ antennas, and each receiver has a single antenna, i.e., $B = 1$. The first three transmitter nodes wish to send 2 independent messages to their corresponding receivers, whereas the remaining three want to send 3 messages, leading to a demands matrix given by $\mathbf{D} = \text{diag}\left[\begin{array}{cccccc} 2 & 2 & 2 & 3 & 3 & 3 \end{array}\right]$. Moreover, 6 channel extensions are used, giving rise to a block-diagonal channel matrix. Following the notation introduced in [28],[16], the scenario of interest corresponds to a $\left[(2 \times 1, 2)^3, (2 \times 1, 3)^3, 6\right]$ interference network with a total of 15 independent streams.

Since the aforementioned system model has been previously studied in [16], we compare the sum-rate slope achieved by homotopy continuation to that obtained by the algorithm in [16], which is denoted here as StructMinIL. This method is a modification of the MinIL algorithm that explicitly enforces a given rank for the signal subspaces while the transmitters satisfy a power budget constraint. Although the StructMinIL method improves the performance of MinIL with symbol extensions, the optimization problem in [16] is non-convex and therefore convergence to the desired solution cannot be guaranteed.

Figure 7 shows the complementary cumulative distribution function (CCDF) of the sum-rate slope achieved by both algorithms at several SNR values. From this figure, it is clear that the DoF performance of HC is better than that of the StructMinIL.

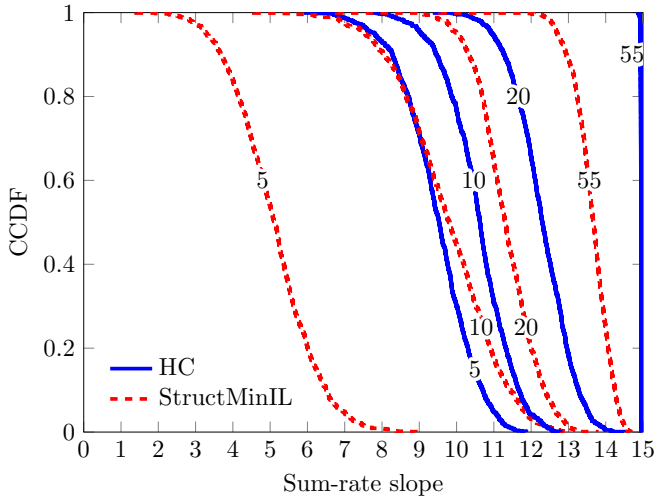

Fig. 7. CCDF of the sum-rate slope at SNR $= \{5, 10, 20, 55\}$ dB in Scenario 4.

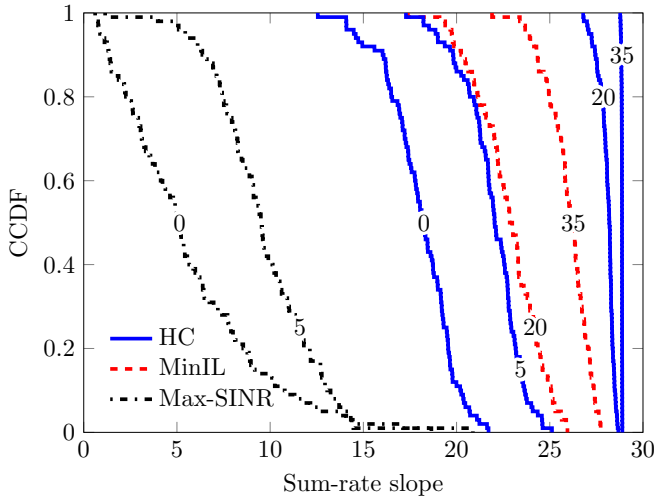

Fig. 8. CCDF of the sum-rate slope at SNR $= \{0, 5, 20, 35\}$ dB in Scenario 5.

Now, we focus on a 2-user X channel, with transmitters having $A_1 = 5$ and $A_2 = 8$ antennas, and with receivers equipped with $B_1 = 6$ and $B_2 = 7$ antennas, respectively. According to [24], this network configuration is capable of transmitting a maximum of 29 independent data streams when using a total of 3 channel extensions. Hereinafter, we will refer to this setting as Scenario 5. The only feasible demands allocation was numerically found to be given by

$$\mathbf{D} = \left[\begin{array}{cc} 5 & 8 \\ 5 & 11 \end{array}\right].$$

The CCDF of the sum-rate slope achieved by HC at different SNR values in Scenario 5 is represented in Fig. 8, which shows that the proposed algorithm always obtains the maximum DoF for SNRs larger than 35 dB, in agreement with the results in [24]. Additionally, we have compared the HC method with two alternative algorithms: for high SNR values (20 and 35 dB) we used again the MinIL method, whereas for low SNR regimes

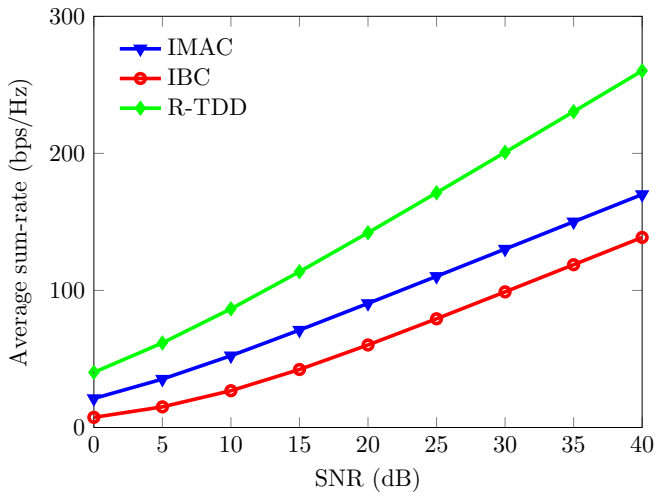

Fig. 9. Average sum-rate achieved by the HC method in three different network configurations.

(0 and 5 dB) we used the maximum signal-to-interference-plus-noise ratio (`Max-SINR`) algorithm [6][45] adapted to work in MIMO X networks. Note that, given the characteristics of `Max-SINR` algorithm, it fits well within the low SNR regime whilst providing a performance similar to `MinIL` for the rest of SNR values. As shown in Fig. 8, the proposed algorithm outperforms both `Max-SINR` and `MinIL` methods, hence being the most appropriate choice for the whole range of SNR values.

C. Cellular networks

The final scenario considered in the simulations comprises $M = 2$ cells, containing $N_1 = 4$ and $N_2 = 3$ users, respectively. In cell 1, the base station (BS) has 12 antennas, whereas each mobile station (MS) is equipped with 8 antennas. Regarding the second cell, its base station has 18 antennas and the mobile stations have 4 antennas each.

In Figure 9, we compare the average sum-rate achieved by the homotopy continuation algorithm in three different configurations of the cellular network: two cells in downlink (IBC), two cells in uplink (IMAC), or cell 1 in downlink and cell 2 in uplink (R-TDD). For both the IBC and IMAC scenarios, in which the two cells operate synchronously as downlink or uplink channels, a maximum of 12 independent, interference-free data streams can be transmitted. However, according to [23], a total of 18 DoF can be achieved by applying the reverse TDD scheme, in which one of the cells operates in downlink mode while the other cell operates in uplink mode. This result is corroborated by our experiments, thus confirming that reverse TDD can enlarge the DoF region in some scenarios.

For the R-TDD scenario, we have further analyzed the probability of attaining the requested number of DoF for the `HC` method in comparison to the `MinIL` algorithm. Homotopy continuation reaches the maximum of 18 streams with a probability of 0.98, while the alternating minimization algorithm is only capable of obtaining the requested DoF with a probability of 0.24. As mentioned in previous sections, the alternating minimization technique often fails to attain the requested DoF in those scenarios where some links act as both desired and interfering link. On the contrary, the `HC` method explicitly considers both (2) and (3), hence achieving the maximum DoF.

TABLE II
AVERAGE NUMBER OF ITERATIONS AND AVERAGE TIME PER ITERATION.

Scenario	Number of iterations		Time per iteration (ms)	
	`HC`	`MinIL`	`HC`	`MinIL`
3	40.55	356.15	43.228	5.788
6 (R-TDD)	314.59	2410.24	66.123	7.200

We finally compare the computational complexity of the `HC` and `MinIL` algorithms. For this comparison, we have considered the X network in Scenario 3 and the reverse TDD mode of Scenario 6. Table II shows the average number of iterations required by each algorithm to achieve convergence in the considered scenarios, as well as the average time per iteration. We can see that the number of iterations for the `HC` method is significantly lower than that of the `MinIL`. However, the average time per iteration is considerably higher[4], resulting in a similar overall convergence time for both algorithms.

VII. Conclusion

In this paper we have presented a new algorithm, based on homotopy continuation, to design interference alignment precoders and decoders for MIMO X networks. The rank constraints on the direct channels are explicitly taken into account and reformulated as new bilinear equations to be solved by the homotopy continuation method together with the conventional interference alignment equations. In this way, the proposed method is able to provide perfect alignment solutions even when time or frequency symbol extensions are used. Unlike competing algorithms, the proposed method has provable convergence guarantees when the IA problem is feasible. Moreover, the proposed algorithm outperforms other existing algorithms, such as the well-known alternating minimization scheme, for a wide variety of channel models including the IC, IBC and IMAC cellular networks, and the X-channel. Finally, the proposed technique has allowed us to provide some insights into the potential benefits of the reverse TDD configuration in comparison to the conventional IMAC and IBC cellular topologies.

Appendix A
Proof of Theorem 1

Our argument is standard in Numerical Algebraic Geometry. We consider the *solution variety*

$$\mathcal{V} = \{(\mathbf{H}_{k\ell}, \mathbf{U}_k, \mathbf{V}_{j\ell}) : (20) \text{ holds}\} \subseteq \mathcal{I} \times \mathcal{O},$$

that is the set of possible pairs $(input, output)$. We also consider the projection $\pi_1 : \mathcal{V} \to \mathcal{I}$. Note that for an input

[4]The average number of Newton corrections for Scenarios 3 and 6 are 3.37 and 4.23, respectively.

$\mathbf{H} = (\mathbf{H}_{k\ell}) \in \mathcal{I}$, the inverse image $\pi_1^{-1}(\mathbf{H})$ of $\mathbf{H}$ by π_1 is just a copy of the set of possible solutions to (20). Of course, that set can be empty.

Lemma 1: Let $(\mathbf{H}, \mathbf{U}_k, \mathbf{V}_{j\ell}) \in \mathcal{V}$, and assume that $(\mathbf{U}_k, \mathbf{V}_{j\ell})$ is a nonsinguar solution of (20) (that is, the linear mapping (21) is invertible). Then, the derivative of π_1 at $(\mathbf{H}, \mathbf{U}_k, \mathbf{V}_{j\ell})$ is invertible.

Proof: First, since (21) is an invertible (thus, surjective) mapping, from the Regular Value Theorem, we have that $\mathcal{V}$ is a smooth manifold in a neighborhood of $(\mathbf{H}, \mathbf{U}_k, \mathbf{V}_{k\ell})$, and the tangent space T to $\mathcal{V}$ at $(\mathbf{H}, \mathbf{U}_k, \mathbf{V}_{j\ell})$ is the set of vectors $(\dot{\mathbf{H}}, \dot{\mathbf{U}}_k, \dot{\mathbf{V}}_{k\ell})$ such that

$$\big(\mathbf{U}_k^T \dot{\mathbf{H}}_{k\ell}(t)\mathbf{V}_\ell + \dot{\mathbf{U}}_k^T \mathbf{H}_{k\ell}(t)\mathbf{V}_\ell + \mathbf{U}_k^T \mathbf{H}_{k\ell}(t)\dot{\mathbf{V}}_\ell\big)_{k,\ell} = 0. \tag{27}$$

The derivative of π_1 sends $(\dot{\mathbf{H}}, \dot{\mathbf{U}}_k, \dot{\mathbf{V}}_{k\ell})$ in T to $\dot{\mathbf{H}}$. Thus, it is surjective (i.e. invertible since the dimensions of $\mathcal{V}$ and $\mathcal{I}$ are equal by assumption) if and only if for any $\dot{\mathbf{H}}$ one can find $(\dot{\mathbf{U}}_k, \dot{\mathbf{V}}_{k\ell})$ satisfying (27). This is clear since the linear mapping (21) is surjective.

■

Note that the solution variety is the zero set of the mapping

$$\begin{array}{rccc} \mathbb{F}: & \mathcal{I} \times \mathcal{O} & \to & \mathbb{C}^b \\ & \big(\mathbf{H}, (\mathbf{U}_k, \mathbf{V}_{j\ell}), \big) & \mapsto & \big(\mathbf{U}_k^T \mathbf{H}_{k\ell} \mathbf{V}_\ell - \mathbf{A}_{k\ell}\big)_{k,\ell} \end{array}$$

We now use [41, Theorem 7.1.1], a somehow classical result in Numerical Algebraic Geometry which follows mainly from Chevalley's Theorem (see for example [46, p. 395]) applied to the projection π_1 and from the Inverse Function Theorem. Instead of recalling [41, Theorem 7.1.1] in its full generality, we just write down its consequence for our problem.

Theorem 2: There exists a non–negative integer $\mathcal{N} \in \mathbb{Z}$ such that for every $\mathbf{H} \in \mathcal{I}$ out of some proper algebraic set Σ, the system $\mathbb{F}\big(\mathbf{H}, (\mathbf{U}_k, \mathbf{V}_{j\ell})\big) = 0$ (with variables $(\mathbf{U}_k, \mathbf{V}_{j\ell})$) has exactly $\mathcal{N}$ nonsingular solutions. Moreover, if $\overline{\mathbf{H}} \in \mathcal{I}$ and if

$$\mathbf{H}(t) = (1-t)\overline{\mathbf{H}} + t\mathbf{H} \notin \Sigma \quad \text{for } t \in (0, 1],$$

then the homotopy $\mathbb{F}\big(\mathbf{H}(t), (\mathbf{U}_k, \mathbf{V}_{j\ell})\big)$ has $\mathcal{N}$ smooth, nonsingular solution paths, and the limit of these paths as $t \to 0$ include all the nonsingular zeros of $\mathbb{F}\big(\overline{\mathbf{H}}, (\mathbf{U}_k, \mathbf{V}_{j\ell})\big)$.

Note that in Theorem 2 we may have $\mathcal{N} = 0$, which corresponds to the case that $\pi_1^{-1}(\mathbf{H}) = \emptyset$ for (almost all) $\mathbf{H} \in \mathcal{I}$, that is the case that the alignment is unfeasible. We also recall [41, Lemma 7.1.2] (adapted to our notation):

Lemma 2: Fix $\overline{\mathbf{H}} \in \mathcal{I}$. Then, for almost all $\mathbf{H} \in \mathcal{I}$, the one–real–dimensional half–open line segment

$$\mathbf{H}(t) = (1-t)\overline{\mathbf{H}} + t\mathbf{H}, \quad t \in (0, 1],$$

is contained in $\mathcal{I} \setminus \Sigma$.

We are now ready to prove Theorem 1.

Proof: In the notations of the theorem, from Lemma 2 for almost all $\mathbf{H} \in \mathcal{I}$ the segment $\mathbf{H}(t)$ does not intersect Σ for $t \in (0, 1]$ (although it might happen that $\mathbf{H}(0) = \overline{\mathbf{H}} \in \Sigma$). From Theorem 2 we then know that there is at least one smooth path $(\mathbf{U}_k(t), \mathbf{V}_{k\ell}(t))$, $t \in (0, 1]$, of nonsingular solutions to $\mathbf{H}(t)$, such that the limit as $t \to 0$ includes $(\overline{\mathbf{U}}_k, \overline{\mathbf{V}}_{k\ell})$. Now, by hypothesis this last is a nonsingular solution of (22), which in particular implies that it is an isolated solution and hence the limit as $t \to 0$ of $(\mathbf{U}_k(t), \mathbf{V}_{k\ell}(t))$ is exactly $(\overline{\mathbf{U}}_k, \overline{\mathbf{V}}_{k\ell})$ (and does not contain more points), so it is a curve which is well–defined in the closed interval $t \in [0, 1]$. On the other hand, from Lemma 1 and the Inverse Function Theorem there exists a local inverse (that we denote by Θ) of π_1 close to $\overline{\mathbf{H}}$ whose image is locally equal to $\mathcal{V}$ in some neighborhood of $(\overline{\mathbf{H}}, \overline{\mathbf{U}}_k, \overline{\mathbf{V}}_{k\ell})$. In other words, for some $\epsilon > 0$ the segment $\mathbf{H}(t)$, $t \in [0, \epsilon)$ can be lifted to $\mathcal{V}$ in a unique way, given by $\Theta(\mathbf{H}(t))$, in such a way that the lift starts at $(\overline{\mathbf{H}}, \overline{\mathbf{U}}_k, \overline{\mathbf{V}}_{k\ell})$. Namely, no more than one of the smooth paths of nonsingular solutions to $\mathbf{H}(t)$ can arrive at $(\overline{\mathbf{H}}, \overline{\mathbf{U}}_k, \overline{\mathbf{V}}_{k\ell})$.

We have proved that there exists a unique solution path $(\mathbf{H}(t), \mathbf{U}_k(t), \mathbf{V}_{k\ell}(t))$ (which, at $t = 1$, defines a unique solution of (20)) that arrives at $t = 0$ to the point $(\overline{\mathbf{H}}, \overline{\mathbf{U}}_k, \overline{\mathbf{V}}_{k\ell})$. One can thereby follow the homotopy backwards, and starting at the known solution at $t = 0$ thus arrive to $t = 1$ getting the solution to the target system $\mathbf{H}$.

■

REFERENCES

[1] Ó. González, J. Fanjul, and I. Santamaria, "Homotopy continuation for vector space interference alignment in MIMO X networks," in *Proc. IEEE Int. Conf. Acoust., Speech, and Signal Process. (ICASSP 2014)*, May 2014, pp. 6232–6236.

[2] S. A. Jafar and S. Shamai (Shitz), "Degrees of freedom region of the MIMO X channel," *IEEE Trans. Inf. Theory*, vol. 54, no. 1, pp. 151–170, Jan. 2008.

[3] M. Maddah-Ali, A. Motahari, and A. Khandani, "Communication over MIMO X channels: interference alignment, decomposition, and performance analysis," *IEEE Trans. Inf. Theory*, vol. 54, no. 8, pp. 3457–3470, Aug. 2008.

[4] V. R. Cadambe and S. A. Jafar, "Interference alignment and degrees of freedom of the K-user interference channel," *IEEE Trans. Inf. Theory*, vol. 54, no. 8, pp. 3425–3441, 2008.

[5] S. Peters and R. Heath, "Interference alignment via alternating minimization," in *Proc. IEEE Int. Conf. Acoust., Speech, and Signal Process. (ICASSP 2009)*, Taipei, Taiwan, Apr. 2009, pp. 2445–2448.

[6] K. S. Gomadam, V. R. Cadambe, and S. A. Jafar, "A distributed numerical approach to interference alignment and applications to wireless interference networks," *IEEE Trans. Inf. Theory*, vol. 57, no. 6, pp. 3309–3322, Jun. 2011.

[7] D. Papailiopoulos and A. Dimakis, "Interference alignment as a rank constrained rank minimization," *IEEE Trans. Sig. Process.*, vol. 60, no. 8, pp. 4278–4288, Aug. 2012.

[8] D. Schmidt, C. Shi, R. Berry, M. Honig, and W. Utschick, "Comparison of distributed beamforming algorithms for MIMO interference networks," *IEEE Trans. Sig. Process.*, vol. 61, no. 13, pp. 3476–3489, Jul. 2013.

[9] I. Santamaria, Ó. González, R. W. Heath, and S. W. Peters, "Maximum sum-rate interference alignment algorithms for MIMO channels," in *Proc. IEEE Global Telecomm. Conference (GLOBECOM 2010)*, Miami, FL, USA, Dec. 2010, pp. 1–6.

[10] H. Yu and Y. Sung, "Least squares approach to joint beam design for interference alignment in multiuser multi-input multi-output interference channels," *IEEE Trans. Sig. Process.*, vol. 58, no. 9, pp. 4960–4966, Sep. 2010.

[11] S. Bazzi, G. Dietl, and W. Utschick, "Interference alignment via minimizing projector distances of interfering subspaces," in *IEEE 13th Workshop Signal Proc. Advances Wireless Comm. (SPAWC 2012)*, Cesme, Turkey, Jun. 2012, pp. 274–278.

[12] ——, "Interference alignment with imperfect channel state information at the transmitter," in *2012 Int. Symposium Wireless Comm. Systems (ISWCS)*, Paris, France, Aug. 2012, pp. 561–565.

[13] G. C. Alexandropoulos and C. B. Papadias, "A reconfigurable iterative algorithm for the K-user MIMO interference channel," *Signal Processing*, vol. 93, no. 12, pp. 3353–3362, Dec. 2013.

[14] Ó. González, C. Lameiro, and I. Santamaria, "A quadratically convergent method for interference alignment in MIMO interference channels," *IEEE Signal Processing Letters*, vol. 21, pp. 1423–1427, Nov. 2014.

[15] P. Mohapatra, K. Nissar, and C. Murthy, "Interference alignment algorithms for the K user constant MIMO interference channel," *IEEE Trans. Sig. Process.*, vol. 59, no. 11, pp. 5499–5508, Aug. 2011.

[16] C. Lameiro, Ó. González, and I. Santamaria, "An interference alignment algorithm for structured channels," in *Proc. IEEE 14th Workshop Signal Proc. Advances Wireless Comm. (SPAWC 2013)*, Darmstadt, Germany, Jun. 2013.

[17] G. Sridharan and W. Yu, "Degrees of freedom of MIMO cellular networks: decomposition and linear beamforming design," *IEEE Trans. Inf. Theory*, vol. 61, no. 6, pp. 3339–3364, Jun. 2015.

[18] C. Suh, M. Ho, and T. D. N. C., "Downlink interference alignment," *IEEE Trans. Comm.*, vol. 59, no. 9, pp. 2616–2626, Sep. 2011.

[19] R. Tresch and M. Guillaud, "Cellular interference alignment with imperfect channel knowledge," in *Proc. IEEE Int. Conf. Comm. (ICC 2009)*, Dresden, Germany, Jun. 2009.

[20] P. Aquilina and T. Ratnarajah, "Performance analysis of IA techniques in the MIMO IBC with imperfect CSI," *IEEE Trans. Comm.*, vol. 63, no. 4, pp. 1259–1270, Apr. 2015.

[21] X. Chu, D. Lopez-Perez, Y. Yang, and F. Gunnarsson, *Heterogeneous Cellular Networks*. Cambridge, 2013.

[22] G. Liu, M. Sheng, X. Wang, W. Jiao, Y. Li, and J. Li, "Interference alignment for partially connected downlink MIMO heterogeneous networks," *IEEE Trans. Comm.*, vol. 63, no. 2, pp. 551–564, Feb. 2015.

[23] K. Kim, S.-W. Jeon, J. Yang, and D. K. Kim, "The feasibility of interference alignment for reverse TDD systems in MIMO cellular networks," Oct. 2014. arXiv: 1410.4624.

[24] A. Agustín and J. Vidal, "Improved interference alignment precoding for the MIMO X channel," in *Proc. IEEE Int. Conf. Comm. (ICC 2011)*, Kyoto, Japan, 2011.

[25] V. R. Cadambe and S. A. Jafar, "Interference alignment and the degrees of freedom of wireless X networks," *IEEE Trans. Inf. Theory*, vol. 55, no. 9, pp. 3893–3908, Sep. 2009.

[26] H. Sun, C. Geng, T. Gou, and S. A. Jafar, "Degrees of freedom of MIMO X networks: spatial scale invariance, one-sided decomposability and linear feasibility," in *Proc. IEEE Int. Symposium Inf. Theory (ISIT 2012)*, Boston, MA: IEEE, Jul. 2012, pp. 2082–2086.

[27] L. Ke, A. Ramamoorthy, Z. Wang, and H. Yin, "Degrees of freedom region for an interference network with general message demands," *IEEE Trans. Inf. Theory*, vol. 58, no. 6, pp. 3787–3797, Jun. 2012.

[28] C. M. Yetis, T. Gou, S. A. Jafar, and A. H. Kayran, "On feasibility of interference alignment in MIMO interference networks," *IEEE Trans. Sig. Process.*, vol. 58, no. 9, pp. 4771–4782, Sep. 2010.

[29] A. Agustín and J. Vidal, "Degrees of freedom region of the MIMO X channel with an arbitrary number of antennas," Oct. 2012. arXiv: 1210.2582.

[30] J. van de Laar, M. Moonen, and P. Sommen, "MIMO instantaneous blind identification based on second-order temporal structure," *IEEE Trans. Sig. Process.*, vol. 56, no. 9, pp. 4354–4364, Sep. 2008.

[31] D. Malioutov, M. Cetin, and A. Willsky, "Homotopy continuation for sparse signal representation," in *Proc. IEEE Int. Conf. Acoust., Speech, and Signal Process. (ICASSP 2005)*, Philadelphia, PA, Mar. 2005, pp. 733–736.

[32] I. Drori and D. Donoho, "Solution of l1-minimization problems by LARS/Homotopy methods," in *Proc. IEEE Int. Conf. Acoust., Speech, and Signal Process. (ICASSP 2006)*, Toulouse, France, May 2006, pp. 733–736.

[33] Ó. González and I. Santamaria, "Interference alignment in single-beam MIMO networks via homotopy continuation," in *Proc. IEEE Int. Conf. Acoust., Speech, and Signal Process. (ICASSP 2011)*, IEEE, May 2011, pp. 3344–3347.

[34] S. R. Krishnamurthy, A. Ramakrishnan, and S. A. Jafar, "Degrees of freedom of rank-deficient MIMO interference channels," *IEEE Trans. Inf. Theory*, vol. 61, no. 1, pp. 341–365, Jan. 2015.

[35] B. Yuan, H. Sun, and S. A. Jafar, "On the optimality of "Half the Cake" for K-user rank-deficient Mk x Mk interference channel," in *IEEE Global Communications Conference (GLOBECOM 2015)*, San Diego, CA, Dec. 2015, pp. 1–5.

[36] J. R. Magnus and H. Neudecker, *Matrix differential calculus with applications in statistics and econometrics*, Third. West Sussex, England: John Wiley & Sons, 1999, p. 450.

[37] H. Sun, C. Geng, T. Gou, and S. A. Jafar, "Degrees of freedom of MIMO X networks: spatial scale invariance, one-sided decomposability and linear feasibility," 2012. arXiv: 1207.6137.

[38] Ó. González, C. Beltrán, and I. Santamaria, "A feasibility test for linear interference alignment in MIMO channels with constant coefficients," *IEEE Trans. Inf. Theory*, vol. 60, no. 3, pp. 1840–1856, Mar. 2014.

[39] C. Garcia and W. Zangwill, *Pathways to solutions, fixed points, and equilibria*. Prentice–Hall, 1981.

[40] T. Y. Li, "Numerical solution of multivariate polynomial systems by homotopy continuation methods," *Acta Numerica*, vol. 6, pp. 399–436, Jan. 1997.

[41] A. J. Sommese and C. W. Wampler II, *The Numerical Solution of Systems of Polynomials Arising in Engineering and Science*. Singapore, Rep. of Singapore: World Scientific Publishing Co. Pte. Ltd., 2005, p. 424.

[42] E. L. Allgower and K. Georg, "Numerical path following," in *Handbook of Numerical Analysis*, August, P. G. Ciarlet and J. L. Lions, Eds., vol. 5, Amsterdam: Elsevier Inc., 1997, pp. 3–207.

[43] Ó. González, C. Beltrán, and I. Santamaria, "On the number of interference alignment solutions for the K-user MIMO channel with constant coefficients," *IEEE Trans. Inf. Theory*, vol. 61, no. 11, pp. 6028–6048, Nov. 2015.

[44] P. Kerret and D. Gesbert, "Interference alignment with incomplete CSIT sharing," *IEEE Trans. Wireless Comm.*, vol. 13, no. 5, pp. 2563–2573, May 2014.

[45] C. Wilson and V. Veeravalli, "A convergent version of the Max SINR algorithm for the MIMO interference channel," *IEEE Trans. Wireless Comm.*, vol. 12, no. 6, pp. 2952–2961, Jun. 2013.

[46] S. Lojasiewick, *Introduction to Complex Analytic Geometry*. Basel–Boston–Berlin: Birkhäuser Verlag, 1991.

Jacobo Fanjul (S'13) received his Telecommunication Engineering (M.Sc.) degree from the University of Cantabria, Santander, Spain, in 2014. In 2013, he joined the Department of Communications Engineering, University of Cantabria, where he is currently pursuing his Ph.D. in Electrical Engineering. During 2016, he was a visiting researcher at the Department of Electrical Engineering and Computer Science (EECS), University of California, Irvine. His current research interests include signal processing algorithms for interference alignment, heterogeneous networks (HetNets), MIMO testbeds and interference management for non-coherent wireless communication.

Óscar González (S'10) received his Telecommunication Engineering Degree and Ph.D. in Electrical Engineering from the University of Cantabria, Santander, Spain, in 2009 and 2014, respectively. During 2012, he was a visiting researcher at the Wireless Networking and Communications Group (The University of Texas at Austin). He has been involved in several national and international research projects on signal processing for wireless communications, interference management/alignment techniques, multiple-input multiple-output (MIMO) systems and wireless communications demonstrators. Currently, he works as a senior data scientist applying machine learning techniques to financial markets. His current research interests include signal processing, machine learning and financial markets modeling.

Ignacio Santamaria (M'96SM'05) received the Telecommunication Engineer degree and the Ph.D. degree in electrical engineering from the Universidad Politecnica de Madrid (UPM), Spain, in 1991 and 1995, respectively. In 1992, he joined the Department of Communications Engineering, University of Cantabria, Spain, where he is currently Full Professor. He has co-authored more than 200 publications in refereed journals and international conference papers, and holds two patents. His current research interests include signal processing algorithms and information-theoretic aspects of multiuser multiantenna wireless communication systems, multivariate statistical techniques and machine learning theories. He has been involved in numerous national and international research projects on these topics. He has been a visiting researcher at the University of Florida (in 2000 and 2004), at the University of Texas at Austin (in 2009), and at the Colorado State University (in 2015). Prof. Santamaria was Technical Co-Chair of the 2nd International ICST Conference on Mobile Lightweight Wireless Systems (MOBILIGHT 2010), Special Sessions Co-Chair of the 2011 European Signal Processing Conference (EUSIPCO 2011), and General Co-Chair of the 2012 IEEE Workshop on Machine Learning for Signal Processing (MLSP 2012). From 2009 to 2014, he was a member of the IEEE Machine Learning for Signal Processing Technical Committee. He served as Associate Editor and Senior Area Editor of the IEEE TRANSACTIONS ON SIGNAL PROCESSING (2011-2015). He was a co-recipient of the 2008 EEEfCOM Innovation Award, as well as coauthor of a paper that received the 2012 IEEE Signal Processing Society Young Author Best Paper Award.

Carlos Beltrán received the Ph. D Degree in Mathematics from the Universidad de Cantabria, Spain, in 2006. He held a postdoctoral fellowship at the U. of Toronto during 2007 and 2008, and is currently a Profesor Titular at the Universidad de Cantabria. He has published around 25 research papers including some which describe a probabilistic solution to Smales 17th problem. He was awarded the Jose Luis Rubio de Francia 2010 prize (Real Sociedad Matemtica Espaola) and the Stephen Smale 2014 prize (Society for the Foundations of Computational Mathematics) for his contributions. He has delivered over 30 talks including several plenaries at different international conferences. His research interests include Numerical Analysis, Complexity and Numerical Algebraic Geometry, as well as applied problems.